Article:
Komissarov, SS orcid.org/0000-0003-4545-9774 (2022) Dynamics of carving runs in alpine skiing. I. The basic centrifugal pendulum. Sport Biomechanics, 21 (8). pp. 890-911. ISSN 1476-3141

https://doi.org/10.1080/14763141.2019.1710559

Dynamics of carving runs in alpine skiing. I. The basic centrifugal pendulum.

Serguei S. Komissarov
Department of Applied Mathematics
The University of Leeds
Leeds, LS2 9JT, UK

Abstract

We studied perfect carving turns of alpine skiing using the simple model of an inverted pendulum which is subject to the gravity force and the force mimicking the centrifugal force emerging in the turns. Depending on the turn speed the model describes two different regimes. In the subcritical regime, there exist three equilibrium positions of the pendulum where the total torque applied to the pendulum vanishes – the marginally stable vertical position and two unstable tilted positions on both sides of the vertical. The tilted equilibria correspond to the ski turns executed in perfect balance. The vertical equilibrium corresponds to gliding down the fall line without turns. In the supercritical regime, the tilted equilibria disappear. In addition to the equilibria, the model allows fall-rise solutions, where the pendulum (skier) rises from the ground on one side and hits the ground on the other side, and solutions describing oscillations about the vertical equilibrium. These oscillations correspond to the so-called dynamic skiing where the skier never settles to a balanced position in the turn. Analysis of the available data on World Cup races shows that elite racers ski mostly in the supercritical regime.

Keywords: alpine skiing, modelling, balance/stability, performance

Introduction

It is often said that proficient alpine skiers ski in a well-balanced position. In the loose casual sense, this simply describes the observations that the skiers do not look to be in danger of falling. In the language of science, this means that the snow reaction force provides sufficient support against the gravity force that pulls the skier down. Moreover, the total torque due to all the forces acting on the skier should be

small or excessive body rotation about its centre of mass (CM) will lead to eventual loss of this support. The latter condition is implicitly accounted in the force diagrams where the vector of the snow reaction force points directly towards the CM or the vector of the force applied by the skier to the snow originates directly from the CM (e.g. LeMaster, 2010).

In perfect carving, the local turning radius of skis is completely determined by the ski sidecut radius $R_{\rm sc}$, which is the radius of the edge of a flatten ski, and the ski inclination angle to the slope Ψ, which is a characteristic of the ski run. Combining this relation with the condition of vanishing torque, one obtains the so-called *Ideal Carving Equation* (ICE), which implicitly determines the balanced inclination angle of the skis (and hence the turn radius) as a function of the turn speed and its angle of traverse (Jentschura & Fahrbach, 2004; Komissarov, 2018). Hence ICE allows to close the system of equations governing the ski turn and describe carving turns in a fully deterministic fashion.

One important feature of this equation is that it imposes both upper and lower limits on the skier speed, which must be satisfied for the balanced inclination angle to exist. If the speed is too low then the upper-C part of the turn cannot be carved unless it stays close to the fall line (Komissarov, 2018). If the speed is too high then in the lower-C part of the turn the centrifugal force dominates the other forces for any inclination angle and throws the skier out of balance (Jentschura & Fahrbach, 2004; Komissarov, 2018). Remarkably, this upper limit

$$V_{\rm sc} = \sqrt{g R_{\rm sc} \cos\alpha} \tag{1}$$

depends only on the sidecut radius of the skis $R_{\rm sc}$ and the local gradient of the ski slope α (g is the constant gravitational acceleration). As the skier speed approaches $V_{\rm sc}$, the combined weight of the skier due to the gravitational and centrifugal forces (the g-force) grows without limit (diverges), making the barrier look impenetrable (Komissarov, 2018).

Let us compare the constraints of quasi-static carving with the performance of elite skiers involved in the World Cup (WC) races organised by the International Ski Federation (FIS) . To this aim we used the data provided in Gilgien, Crivelli, Spörri, Kröll, and Müller (2015) for GS (giant slalom), SG (super-giant slalom) and DH (downhill) competitions and in Supej, Hebert-Losier, and Holmberg (2014) for SL (slalom) competitions. The data presented in (Gilgien et al., 2015) are based on the races during the 2010/2011 and 2011/2012 seasons, fourteen GS runs, four SG and four DH runs altogether. These were made by forerunners before the start of the actual race. The data of Supej et al. (2014) are based on the runs by ten actual participants of a WC race held in Kranjska Gora, Slovenia. The season is described in the paper as 'current', presumably 2014/2015. Table 1 shows some of the measured parameters which we find directly relevant to our study (We have reduced the number of significant digits compared to the original, keeping only as many as needed for the purpose.). These are the ski sidecut radius $R_{\rm sc}$, the slope gradient angle α, the mean

Table 1
Parameters of race runs (Gilgien et al., 2015; Supej et al., 2014). R_{sc} is the sidecut radius of skis, α is the inclination angle of the slope, $\langle L_v \rangle$ and $\langle L_h \rangle$ are the mean separations between the gates down the fall line and across the fall line respectively, R_a is the radius of the arc defined by the mean gate separations, V is the skier speed, $\zeta = \langle V \rangle^2 / g R_{sc}$ is a dimensionless speed parameter and L_g is the distance along the fall line required to reach the speed $\langle V \rangle$.

Parameter	SL	GS	SG	DH
R_{sc} [m]	≤ 15	27	33	45
α [°]	22 ± 3	18 ± 7	17 ± 7	14 ± 8
$\langle L_{\mathrm{v}} \rangle$ [m]	12	25	48	74
$\langle L_{\mathrm{h}} \rangle$ [m]	4	7	12	29
R_{a} [m]	9.0	20	45	52
V [m/s]	12±1	18±2	24±3	26±4
$L_{\mathrm{g}}/\langle L_{\mathrm{v}} \rangle$	1.6	2.1	2.1	1.9
ζ	≥1.0	1.2	1.8	1.5

separations of the gates along and across the fall line, $\langle L_{\mathrm{v}} \rangle$ and $\langle L_{\mathrm{h}} \rangle$ respectively, the turn radius dictated by the gate separation R_{a}, the recorded speed V and the speed parameter

$$\zeta = \langle V \rangle^2 / g R_{\mathrm{sc}} \, .$$

Unfortunately, Gilgien et al. (2015) do not state the sidecut radii of the forerunners skis and we simply adopted the minimum radii allowed by FIS regulations in force for the seasons. This is quite reasonable as most racers actually prefer skis with the smallest allowed sidecut radius. Similarly, Supej et al. (2014) only state that the upper limit on R_{sc} was 15m. The gate-dictated turn radius R_{a} was calculated using the equation (28) derived in Appendix B, where we put $L = \langle L_{\mathrm{v}} \rangle$ and $H = \langle L_{\mathrm{h}} \rangle + \Delta$. Here the offset parameter Δ accounts for horizontal separation between the turning pole and skis at gate passing. We used $\Delta = 2\,\mathrm{m}$ for GS, SG and DH and $\Delta = 0.6\,\mathrm{m}$ for SL.

One can see that in the SL, GS and SG races the mean slope gradient is significantly higher than the critical one, where the speed of ideal carving runs approaches V_{sc} (Komissarov, 2018). In the DH races, the mean gradient is almost the same as the critical one but the standard deviation given for slope gradient shows that the DH tracks include much steeper sections. Thus we conclude that the ideal carving as described by Komissarov (2018) should not be possible on these race tracks.

Moreover, the skier's mean speed is systematically exceeding the upper speed limit of ideal carving. This is nicely illustrated by the fact the the parameter $\zeta = \langle V \rangle^2 / g R_{\mathrm{sc}}$ is higher than unity. Note that $g R_{\mathrm{sc}}$ exceeds V_{sc}^2 by the factor $1/\cos\alpha$ which is close to unity. Although the available SL data do not exclude the possibility of ζ being close to unity, this is still too extreme as V_{sc} is a theoretical limit for ideal

carving which is not expected to be reached in real skiing. Somehow the elite racers manage to ski faster than the theory of ideal carving predicts.

DH tracks typically include long gliding/traversing sections where the speed is significantly higher than in the sections which force skiers to turn. For example, Clarey's record speed $v = 45\,\mathrm{m/s}$ is almost twice as much as the mean speed given in Table 1. To a lesser degree this is also true for SG tracks, which are normally set on the same slopes as DH tracks. The high speed of such sections may well be the reason behind the high mean values. The fact that the mean turn radius dictated by the gates R_a is comparable or even larger than R_sc in SG and DH (see Table 1) is consistent with this explanation. At the end of gliding sections, SG and DH racers tend to execute skidded turns. Since the speed limit V_sc is not applicable to skidded turns, they seem to be a reasonable option when the entry speed is significantly higher. The enhanced friction of skidded turns results in a significant speed reduction presumably down to the level allowing quasi-static carving later on. This explanation requires further investigation in order to access its validity.

In contrast, GS and SL runs are dominated by turns. This is illustrated by the fact that the turn radius dictated by the gates, R_a, is significantly smaller than the sidecut radius of the skis. Hence the high speed of these races requires a different explanation. The hybrid turns, with initial pivoting and skidding followed by carving, are typical in these disciplines. As we have discussed earlier the kinetic energy dissipation associated with skidding can keep the speed below V_sc, allowing the finishing carving turn phase even when the slope gradient exceeds the critical one (Komissarov, 2018), as it often does on GS and SL tracks. However, this explanation is in conflict with the observed speeds exceeding V_sc.

Here we critically revise the model of ideal carving and investigate if its assumptions are too restrictive. In particular, we focus our attention on the condition of zero torque. Indeed, this condition implies a quasi-static body position during the turn combined with dynamic transitions between the turns, whereas we often see good skiers effortlessly moving from turn to turn in a smooth continuous and rhythmic fashion. These movements are very reminiscent of a metronome or a inverted pendulum.

Morawski (1973) already described the skier motion using the model of inverted pendulum, whose pivot point is allowed to slide horizontally. The pendulum can be prevented from hitting the floor via a control force applied at the pivot point and pushing it the direction where the pendulum is leaning. While the ski sideslipping and edging are named as the ways of applying the control force in skiing, their mathematical model is rather abstract, with the equation of the control force postulated and not derived from detailed analysis of the interaction between the ski and the snow. Finally, the pendulum equation is linear and hence suitable only for small deviations from the equilibrium position.

In this paper, we return to the pendulum model but instead of focusing on the control side of the problem we study the natural motion of the pendulum driven

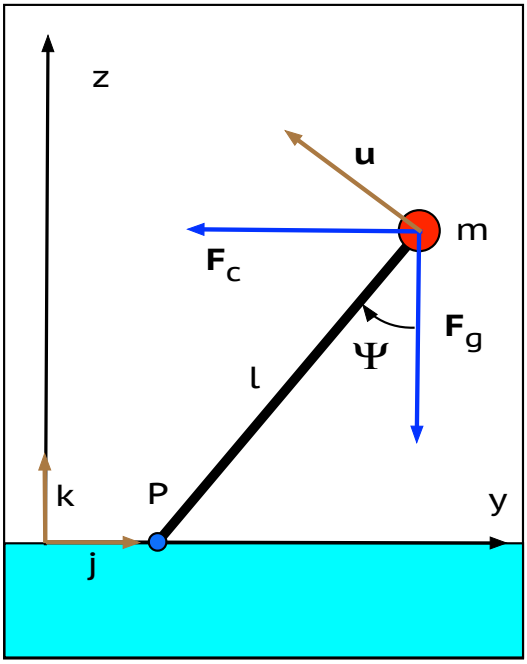

Figure 1. Inverted pendulum. A leg of constant length l is attached to the pivot joint P affixed to the ground. A mass m is affixed to the other end of the leg. The mass is subject to the gravity force $\boldsymbol{F}_{\mathrm{g}}$ pointing vertically downwards and the horizontal force $\boldsymbol{F}_{\mathrm{c}}$ corresponding to the centrifugal force experienced by the skier. Vector $\boldsymbol{u}$ is the velocity of the mass and Ψ is the angle between the leg and the vertical direction.

by the gravitational force and the centrifugal force naturally emerging in the limit of carving turns with zero side-slipping. Since the pendulum naturally allows oscillatory solutions which do not satisfy the condition of force balance underpinning ICE, we hypothesise that this may allow us to overcome its upper speed limit and provide a better theoretical model for performance skiing.

Methods

The basic model of centrifugal pendulum

The key assumption of the ideal carving turn is that at every point of the turn the skier is in balance. This includes the condition of zero torque, which defines the skier inclination angle. However, we have seen that during the turn the balanced inclination angle varies significantly, particularly on steeper slopes. Hence, in reality the balance must be only approximate as otherwise the angle would remain unchanged. In this section we explore the potential implications of the deviation from the torque balance to the speed of carving turns. To this aim we will use a simple model of forced inverted pendulum, corresponding to the skier pivoting about the edges of their skis.

The problem is illustrated in Figure 1. A mass m is affixed to the upper end of

a massless solid rod of length l whose lower end is attached to a stationary pivot point P on a flat horizontal surface. Normally the model of inverted pendulum allows the pivot point to move under the action of external forces and the motion is analysed using an inertial frame of reference associated with the ground. Here we prefer to use the non-inertial (accelerated) frame of reference co-moving with the pivot point. This accelerated motion of the frame gives rise to the inertial force acting on the pendulum weight. In the context of skiing, the pivot point is identified with the edged skis, l with the distance between the skier centre of mass (CM) and the ski edge and m with the total mass of the skier and their equipment. The non-inertial force of the pendulum corresponds to the centrifugal force experienced by the skier.

To describe the pendulum motion quantitatively, we use Cartesian coordinate with the origin at the pivot point and the basis vectors $\boldsymbol{i}$, $\boldsymbol{j}$ and $\boldsymbol{k}$, such that the pendulum moves in the plane orthogonal to $\boldsymbol{i}$ and $\boldsymbol{k}$ points upwards in the vertical direction. The position vector $\boldsymbol{r}$ connects the origin with the affixed mass. The inclination angle Ψ is the angle between the vertical direction and the pendulum. We agree that it is positive in the clockwise direction and negative in the anti-clockwise direction (see Figure 1).

The mass is subject to the vertical gravity force $\boldsymbol{F}_{\mathrm{g}} = -mg\boldsymbol{k}$ and the centrifugal force

$$\boldsymbol{F}_{\mathrm{c}} = \begin{cases} -(mV^2/R)\boldsymbol{j} & \text{if} \quad \Psi > 0; \\ 0 & \text{if} \quad \Psi = 0; \\ +(mV^2/R)\boldsymbol{j} & \text{if} \quad \Psi < 0. \end{cases} \tag{2}$$

where V is the skier speed and R is the curvature radius of the ski trajectory. For a perfect carving turn on hard snow

$$R = R_{\mathrm{sc}} \cos \Psi \tag{3}$$

(Howe, 2001; Lind & Sanders, 1996). Strictly speaking, this relation is based on the assumption that the penetration of the snow surface by the skis is negligibly small. If however it is significant, it is important to know how the penetration depth is distributed along the ski. As most of the pressure is loaded on the snow under the skier foot, one may expect the penetration to be deepest at the ski midpoint, leading to somewhat shorter value of R (Howe, 2001). (Although due to the snow plasticity, we would expect the same penetration depth at the ski tail, it should still decrease towards the shovel.) If some degree of skidding was involved then one would expect to find a larger value of R instead (Mössner, Heinrich, Kaps, Schretter, & Nachbauer, 2009; Yoneyama, Kagawa, & Funahashi, 2002) . For simplicity, we ignore these caveats here.

The discontinuous nature of F_{c} arises from the fact that when the ski is only slightly tilted relative to the slope surface it starts carving an arc with its side-cut radius R_{sc}. Only if the ski is flat on the snow it may glide without turning – we will come back to the gliding case later in the paper. Obviously, the model corresponds to

the simplified case of vanishingly small slope gradient. This and other simplifications of the model can be gradually removed in future investigations.

The swinging of the pendulum is governed by the equation

$$\frac{d\boldsymbol{M}}{dt} = \boldsymbol{K}\,, \tag{4}$$

where $\boldsymbol{M} = m\boldsymbol{r}\times\boldsymbol{u}$ is the pendulum angular momentum and $\boldsymbol{K} = \boldsymbol{r}\times\boldsymbol{F}_{\mathrm{g}} + \boldsymbol{r}\times\boldsymbol{F}_{\mathrm{c}}$ is the total torque about the pivot point (Landau & Lifshitz, 1969). The position vector $\boldsymbol{r} = l\sin\Psi\boldsymbol{j} + l\cos\Psi\boldsymbol{k}$, and the velocity vector $\boldsymbol{u} = l(d\Psi/dt)(\cos\Psi\boldsymbol{j} - \sin\Psi\boldsymbol{k})$ (not to be confused with the ski speed V). Upon the substitution of all these expressions, equation (4) reduces to

$$\frac{d^2\Psi}{dt^2} = \frac{g}{l}\sin\Psi - \frac{V^2}{lR_{\mathrm{sc}}}\operatorname{sgn}\Psi\,, \tag{5}$$

where

$$\operatorname{sgn}\Psi = \begin{cases} +1 & \text{if} \quad \Psi > 0; \\ 0 & \text{if} \quad \Psi = 0; \\ -1 & \text{if} \quad \Psi < 0. \end{cases}$$

is the sign function. This second order ordinary differential equation is the dynamic equation describing the motion of the pendulum. The right-hand side of this equation is a continuous function everywhere except $\Psi = 0$. Therefore it allows solutions in the extended sense compared to the Peano's existence theorem (Coddington & Levinson, 1955). Their first derivative is an absolutely continuous function.

Via introducing the dimensionless time $\tau = t\sqrt{g/l}$ equation (5) is reduced to its basic form

$$\frac{d^2\Psi}{d\tau^2} = \sin\Psi - \zeta\operatorname{sgn}\Psi\,, \tag{6}$$

where $\zeta = V^2/gR_{\mathrm{sc}}$ is the same speed parameter as in Table 1. The first term on the right side of the equation represents the torque due to gravity and the second one the torque due to the centrifugal force.

Trajectories of carving runs

How to reproduce the trajectory or ski runs using our simple model of centrifugal pendulum? This is a rather complicated problem and here we will follow the simplified approach by Morawski (1973). Hence we assume that the ski slope is flat and horizontal, with the z axis normal to the slope plane and the x axis pointing in the direction of the run. We will also ignore all energy losses and hence assume that the skier speed is constant.

Equation (5) governs the evolution of the ski tilt angle. This angle allows us to find the local curvature radius of the ski trajectory $R = R_{\mathrm{sc}}\cos\Psi$ and hence the rate

at which the traverse angle of the trajectory γ varies in time

$$\frac{d\gamma}{dt} = \frac{V}{R_{\rm sc}} \frac{\rm sgn\,\Psi}{\cos\Psi}\,. \tag{7}$$

The traverse angle defines how the skis moves in the slope plane via

$$\frac{dx}{dt} = V\cos\gamma\,, \qquad \frac{dy}{dt} = V\sin\gamma\,, \tag{8}$$

where $x(t)$ and $y(t)$ are the ski coordinates. The trajectory of the skier CM can then be found via

$$x_{\rm S}(t) = x(t)\,, \quad y_{\rm S}(t) = y(t) + l\sin\Psi(t)\,. \tag{9}$$

In this problem, there is a natural length scale $\mathcal{L} = R_{\rm sc}$ and the time scale $\mathcal{T} = R_{\rm sc}/V$. These lead to the dimensionless equations

$$\frac{d^2\Psi}{ds^2} = \delta(\zeta^{-1}\sin\Psi - \ {\rm sgn}\,\Psi)\,, \tag{10}$$

$$\frac{d\gamma}{ds} = \ {\rm sgn}\,\Psi\sec\Psi\,, \tag{11}$$

$$\frac{d\bar{x}}{ds} = \cos\gamma\,, \tag{12}$$

$$\frac{d\bar{y}}{ds} = \sin\gamma\,, \tag{13}$$

where $s = t/\mathcal{T}$, $\bar{x} = x/R_{\rm sc}$, $\bar{y} = y/R_{\rm sc}$ and the dimensionless parameter $\delta = R_{\rm sc}/l$.

Results

Types of solutions of the pendulum equation

The types of solutions allowed by pendulum equation (6) depend on the value of ζ. To elucidate this we convert it in the following equivalent system of first-order equations

$$\begin{aligned} \frac{d\Omega}{d\tau} &= \sin\Psi - \zeta\,{\rm sgn}\,\Psi \\ \frac{d\Psi}{d\tau} &= \Omega\,, \end{aligned} \tag{14}$$

where Ω is the angular velocity of the pendulum, and build its phase portraits for $\zeta < 1$ and $\zeta > 1$. Figure 2 gives two representative examples of such portraits. Their lines show the tracks (or orbits) of particular solutions. As the time increases the point representing the system moves along the orbit. Some of the orbits are closed and correspond to the rhythmic oscillations of the pendulum. Others originate and terminate at $\Psi = \pm 90^\circ$. These describe the pendulum being released from the ground

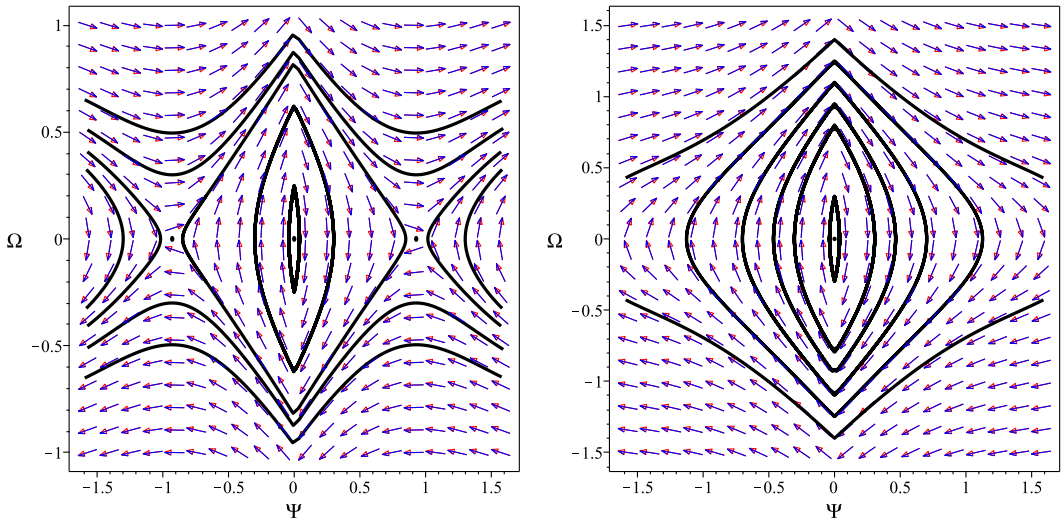

Figure 2. Phase portraits of the pendulum equation (6) for $\zeta = 0.8$ (left) and $\zeta = 1.2$ (right).

and then hitting the ground again. Depending on the angular velocity at the release, it either comes back to the same side of the pivot or goes over the pivot and hits the ground on the other side. The arrows shows the direction of time evolution, but not its rate, throughout the whole domain.

In both cases, the phase portraits include the equilibrium point $\Psi = \Omega = 0$ (the central black dots in Figure 2). It corresponds to marginally stable vertical position of the pendulum and the gliding option in skiing. Small deviations from this equilibrium result in oscillations around the vertical position, which correspond to the closed orbits around the centre in the portraits. In the theory of dynamical systems such points are called centres.

When $\zeta < 1$ (the subcritical regime), the system allows two more equilibrium points, $(\Psi_{\text{eq}}, \Omega) = (\pm \arcsin \zeta, 0)$. In the left panel of Figure 2 these show up as the two off-centred black dots on the Ψ axis. At these points the total torque acting on the pendulum vanishes – they correspond to the left and right turns of quasi-static carving. Any deviation from such equilibrium puts the system on an orbit moving away from the equilibrium and hence this equilibrium is unstable (cf. Komissarov, 2018). In the theory of dynamical systems such equilibrium points are called saddles. The phase orbits approaching the equilibrium from above, from below or from the far side eventually terminate at $\Psi = \pm\pi/2$ (or $\pm 90°$). This corresponds to the pendulum (skier) falling. However, the orbits closer to the centre point are closed and correspond to the metronome regime of the pendulum. In skiing this must correspond to a rhythmic chain of dynamic carving turns.

In the supercritical regime ($\zeta > 1$), which is the case for the FIS WC races, the saddle points disappear and hence the balanced carving is no longer possible.

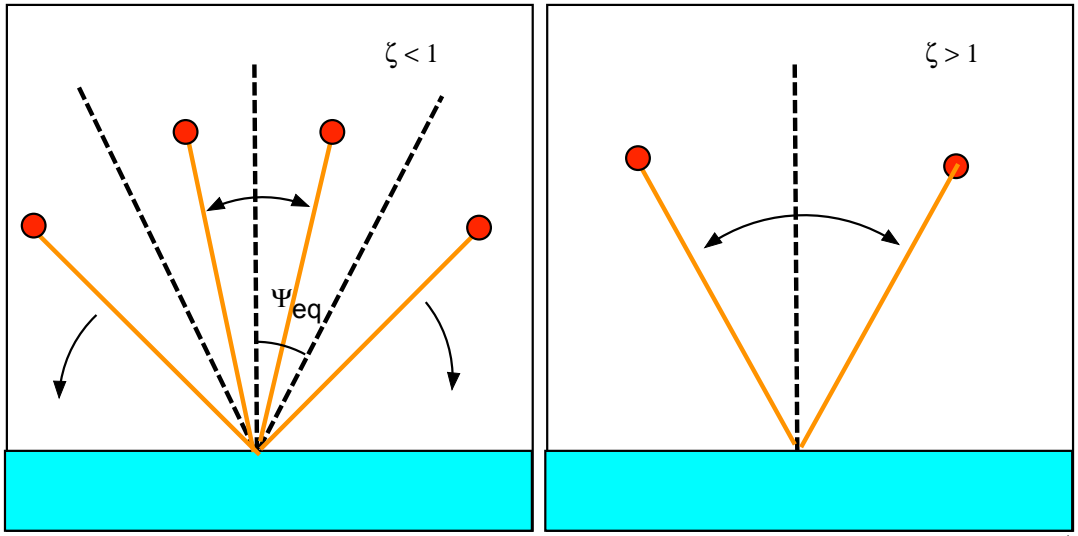

Figure 3. The two configurations of the centrifugal pendulum. When $\zeta < 1$ (left panel) there are three static positions of the pendulum – the vertical one and the two inclined at $\Psi = \Psi_{\rm eq}$ to the both sides of the vertical. When $\zeta > 1$ (right panel) only the vertical one remains.

However, the centre remains and so do the closed orbits around it. Hence the rhythmic carving turns are still possible but during these turns the skier is never in balance. The crash solutions are also retained. The solution type is determined by the pendulum angular velocity at the vertical position. The crash occurs when it exceeds the critical value of $\Omega_{\rm crash} = \zeta\pi - 2$.

Figure 3 illustrates the two different regimes of the centrifugal pendulum. If $\zeta < 1$ the pendulum can remain motionless when put in the vertical position or at the inclination angle $\Psi_{\rm eq}$ to the vertical. When put in the position with $\Psi < \Psi_{\rm eq}$ and released it begins to oscillate about the vertical position. If however the initial inclination exceeds $\Psi_{\rm eq}$ it falls to the ground. As ζ increases, so does $\Psi_{\rm eq}$, which reaches 90° at $\zeta = 1$. When $\zeta > 1$ only the vertical static position remains and the pendulum oscillates when released at any inclination.

Phase portraits are very useful for identifying all types of solutions allowed by the dynamical system. However, they do not show the speed at which the point representing a particular solution moves along its orbit. In order to clarify this aspect of the problem we prepared Figure 4 which shows a number of particular solutions $\Psi(\tau)$ satisfying the initial conditions $\Psi(0) = \Psi_{\rm max}$ and $\Omega(0) = 0$. For oscillatory solutions, $\Psi_{\rm max}$ gives their amplitude. One can see that both for $\zeta < 1$ and for $\zeta > 1$, the smaller amplitude implies the shorter period of the pendulum oscillation and hence shorter duration of the carving turn. The plot for $\zeta = 0.8$ reveals additional interesting information. In the plot, the horizontal line corresponds to the equilibrium solution $\Psi_{\rm eq} = \arcsin\zeta$. Formally, it corresponds to the infinite period. As to the

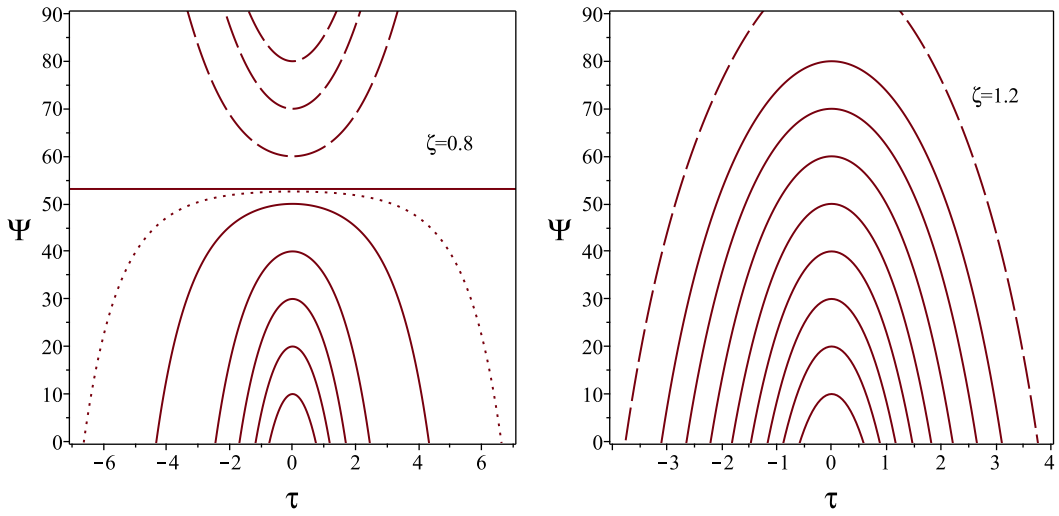

Figure 4. Solutions to the pendulum equation (6) with $\zeta = 0.8$ (left) and $\zeta = 1.2$ (right). They all satisfy the initial conditions $\Psi(0) = \Psi_{\max}$ and $d\Psi/d\tau(0) = 0$. Both the panels include curves corresponding to $\Psi_{\max} = 10$, 20, 30, 40, 50, 60, 70 and 80 degrees (solid lines). The left panel also shows the equilibrium solution $\Psi = \Psi_{\rm eq} = \arcsin\zeta$ and the solution corresponding to $\Psi_{\max} = 0.99\Psi_{\rm eq}$ (dotted line). The right panel also shows the solution corresponding to $\Psi_{\max} = 100°$. The 'crash' solutions, which hit $\Psi = 90°$ are indicated using dashed lines.

other solutions their period grows without limit as $\Psi_{\max}$ approaches $\Psi_{\rm eq}$.

The limit of small amplitude

For small inclination angles, $\Psi \ll \zeta$, equation (6) reduces to the simple linear equation

$$\frac{d^2\Psi}{d\tau^2} = -\zeta\,\mathrm{sgn}\,\Psi\,. \tag{15}$$

This equation has periodic solutions with the period

$$P = 4\sqrt{2}\left(\frac{\Psi_{\max}}{\zeta}\right)^{1/2}\,. \tag{16}$$

Defining $\tau = 0$ as the time of passing over the vertical position (the switching point between turns), one cycle of such solutions is

$$\Psi = \begin{cases} +(\zeta/2)\tau^2 + \dot\Psi_0\tau & \text{if} \quad -P/2 < \tau \le 0\,; \\ -(\zeta/2)\tau^2 + \dot\Psi_0\tau & \text{if} \quad 0 < \tau < P/2\,, \end{cases} \tag{17}$$

where

$$\dot\Psi_0 = \sqrt{2\zeta\Psi_{\max}}$$

is $\dot{\Psi}$ at $\tau = 0$. These vibrations of the pendulum suggest a model for the fall line gliding on carving skis where it is not a perfectly straight run but is made out of little arcs of the radius $R_{\rm sc}$ instead.

The snow contact condition

As the pendulum's weight is attached to the pivot point with a solid rod it can never be catapulted into the air. This not necessarily true for skiers who can lose contact with the snow even when running down a perfectly flat slope. Since in reality it is the gravity force that keeps the skier on the slope, we need to check that in the pendulum solution the negative vertical acceleration of the weight does not exceed the gravitational acceleration. Differentiating $z = l\cos\Psi$ twice with respect to t, dividing the result by g and introducing the dimensionless time variable τ as before, we find that the ratio of the accelerations

$$a_{\rm Z}/g = -\cos(\Psi)\dot{\Psi}^2 - \sin(\Psi)\ddot{\Psi}\,,$$

where $\dot{a}$ stands for the derivative with respect to τ. Upon the substitution of the expression for $\ddot{\Psi}$ given by equation (6), this reads

$$a_{\rm Z}/g = -\cos(\Psi)\dot{\Psi}^2 - \sin^2\Psi + \zeta|\sin\Psi|\,. \tag{18}$$

Using the energy conservation law derived in Appendix A, one finds that

$$\dot{\Psi}^2 = 2\left((\cos\Psi_{\rm max} - \cos\Psi)\right) + \zeta(\Psi_{\rm max} - \Psi)\,, \tag{19}$$

which allows us to define $a_{\rm Z}$ as a function of Ψ and $\Psi_{\rm max}$. An example of this function is shown in the left panel of Figure 5. One can for all solutions, parametrised by the value of $\Psi_{\rm max}$, the peak of the negative acceleration occurs at the summit point ($\Psi = 0$). Although, we have not been able to prove that this is always the case, our numerical exploration of $a_{\rm Z}(\Psi, \Psi_{\rm max})$ for a number of values of the speed parameter ζ suggests that for all oscillatory solutions $a_{\rm Z}$ has an absolute minimum at the summit.

Demanding $a_{\rm Z}/g > -1$ at the summit ($\Psi = 0$) we arrive to the condition

$$\dot{\Psi}^2(0) < 1\,. \tag{20}$$

Since at the summit

$$\dot{\Psi}^2(0) = 2(\cos(\Psi_{\rm max}) + \zeta\Psi_{\rm max} - 1)\,,$$

we can rewrite condition (20) as

$$\zeta < \zeta_{\rm max}\,, \quad \text{where} \quad \zeta_{\rm max} = \frac{3 - 2\cos(\Psi_{\rm max})}{2\Psi_{\rm max}}\,. \tag{21}$$

The white area of the diagram in right panel of figure 5 shows the region of the $(\Psi_{\rm max}, \zeta)$ plane where $\zeta < \zeta_{\rm max}$ and $\Psi_{\rm max}$ is below the upper limit set by

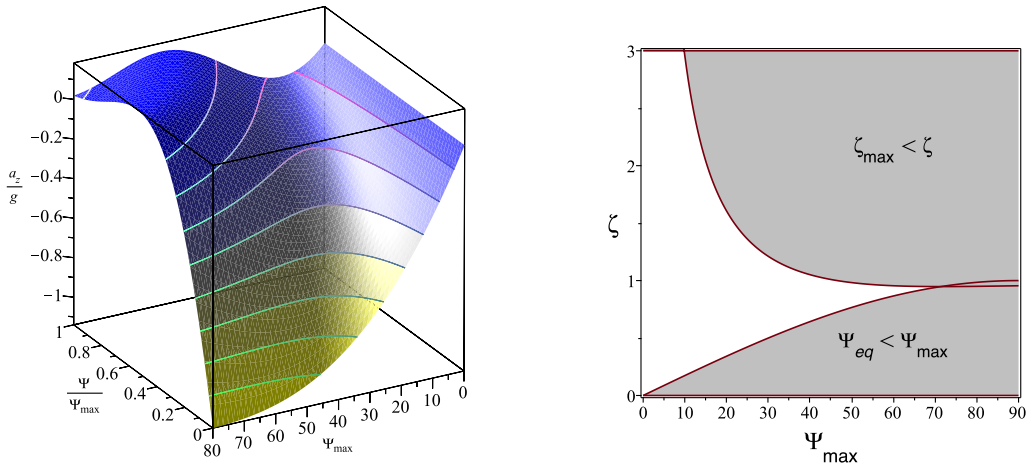

Figure 5. The left panel shows the function $a_{\mathrm{Z}}(\Psi, \Psi_{\max})$ for $\zeta = 1$. In this image, the discrete gradation of colour is used to visualise the lines of equal a_{Z}. For all values of $\Psi_{\max}$, the (negative) acceleration peaks at $\Psi = 0$. The right panel illustrates the limitations imposed on the amplitude of the pendulum oscillations. In the upper shaded area, the snow contact condition is not satisfied. In the lower shaded area, the amplitude exceeds the upper limit set by the equilibrium value $\Psi_{\mathrm{eq}}(\zeta)$.

the equilibrium solution $\Psi_{\mathrm{eq}} = \arcsin\zeta$. One can see that in the subcritical regime ($\zeta < 1$) the snow contact is almost aways preserved. In the supercritical regime ($\zeta > 1$), permanent snow contact is only possible for turns with small inclination. According to the model, the skier would be catapulted into the air when exiting a turn with a sufficiently high inclination angle. Surely this is not what we see in the practice of FIS WC racing and the finding means that we have identified a limitation of our basic model. Most likely, this limitation originates from the assumption of fixed pendulum length, whereas even advanced recreational skiers routinely flex and extend their legs when making turns. Flexing legs on approach to the summit point (transition between turns) softens the upward push of CM.

Properties of the trajectories

For simplicity, the runs are initiated by the conditions $\bar{x}(0) = 0$, $\bar{y}(0) = 0$, $\gamma(0) = 0$, $d\Psi/ds(0) = 0$ and $\Psi(0) = \Psi_{\max}$. No matter what the dimensional parameters of the problem are, if the dimensionless parameters ζ and δ are the same then so is the dimensionless trajectory $\bar{y} = f(\bar{x})$. The dimensional trajectory can then be obtained via multiplication by the scaling factor $\mathcal{L}$.

Figure 6 shows one example where the solid line indicates the trajectory of a skier CM and the dotted line the trajectory of skis. In all our numerical models we calculate the value of δ using $l = 1\,\mathrm{m}$.

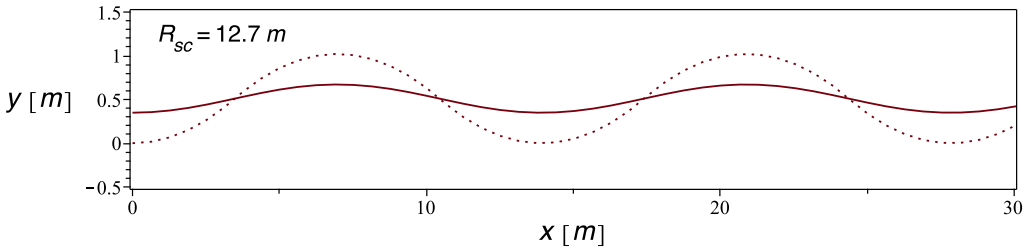

Figure 6. An example of simulated ski runs. The parameters are $\zeta = 1$, $\delta = 12.7$, $\Psi_{\max} = 20°$. The solid line show the trajectory of the CM and the dotted line the trajectory of skis.

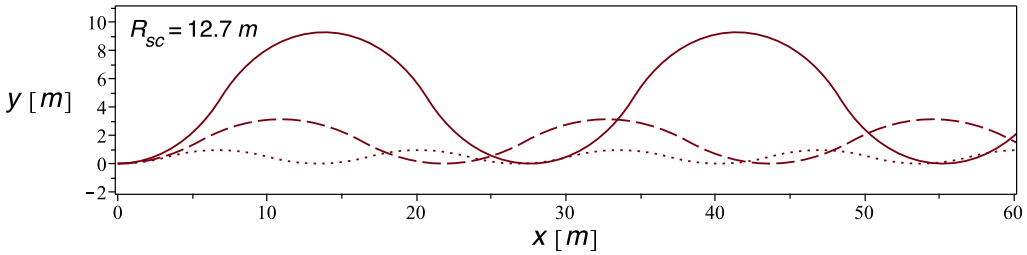

Figure 7. Dependence of the carving runs on the peak inclination angle. The curves correspond to $\Psi_{\max} = 60°$ (solid line), $\Psi_{\max} = 40°$ (dashed line) and $\Psi_{\max} = 20°$ (dotted line).

Figure 7 shows the ski trajectories of carving runs for $R_{\rm sc} = 12.7\,\mathrm{m}$, $V = 12\,\mathrm{m/s}$ ($\zeta = 1.18$) and $\Psi_{\max} = 20°$, $40°$ and $60°$. As $\Psi_{\max}$ increases the turn duration increases as well and so does the length of the turn. Moreover, higher Ψ means shorter curvature radii of the trajectory (see Eq.3) and so the increase of $\Psi_{\max}$ also results in the turns becoming wider, with stronger deviation from the fall line.

Quasi-static runs

In order to compare these results with the trajectories of runs made near the static limit, we considered a model with the speed reduced to $7\,\mathrm{m/s}$ ($\zeta = 0.39$) and $\Psi_{\max} = 0.99\Psi_{\rm eq} = 23°$. The result is shown in Figure 8. One can see that the turns are significantly longer and wider than in the dynamic run of Figure 7 with similar amplitude $\Psi_{\max}$. In fact, they are longer and wider even than in the dynamic run with $\Psi_{\max} = 60°$. This is because the quasi-static solution spends a long time near $\Psi_{\rm eq}$ (see Figure 4), which allows it to deviate significantly from the fall line before entering the transition phase.

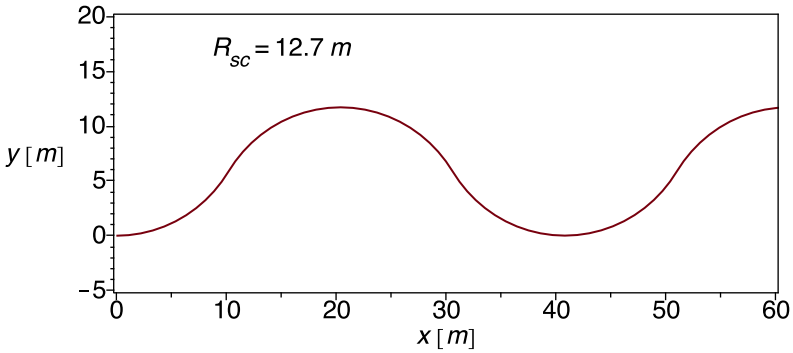

Figure 8. A quasi-static run with $\Psi_{\max} = 0.99\Psi_{\rm eq}$.

Model versus race data

Now we compare our highly simplified model with the real races using the data presented in Table 1 to see its potential for describing the skiing by top athletes, to check if it is any good and if it is then in which racing disciplines.

We start by noticing that the dependence between the amplitude and period of the centrifugal pendulum (see figure 4) can be quickly converted into the dependence between the peak inclination $\Psi_{\max}$ and the length of the turn L. In fact, all we have to do is to multiply the half period of the solution with given $\Psi_{\max}$ first by the time scale $\mathcal{T} = \sqrt{l/g}$ and then by the relevant speed scale V. The results can than be compared with the mean distance between the gates of the race courses.

Figure 9 shows the predicted $L(\Psi_{\max})$ for the SL and GS runs, using $l = 1\,m$ ($\mathcal{T} \approx 0.32\,$s) and the values of V and ζ from Table 1. In the left panel we have the results obtained with $\zeta = 1$, which is more suitable for the SL runs. Hence, the GS results are shown only for comparison. According to the panel, the mean separation between the gates, $\langle L \rangle = 12.6\,$m, is inside the range of the turn lengths predicted by the model. In fact, the two lengths match each other when $\Psi_{\max} \approx 40°$. Unfortunately, Supej et al. (2014) do not give the mean value of this angle. Instead they give the data for the hip angulation, which show that it peaks at about 40°. This angle would be the same as the ski inclination angle if the skier's torso remained vertical. If however the torso was inclined to the slope in the same sense as the skier's legs, which is typically the case, then the ski inclination would be higher. The study also presents the data for the radius of the ski trajectory which bottoms out at about $R_{\min} =$ 6-7 m. Assuming that skis are carving at this phase of the turn, we can apply formula (3) and obtain $\Psi_{\max} = 62°$ - 66° which is indeed higher than our theoretical estimate. In a similar field study of kinematics and dynamics of actual SL runs, it was also found that the ski inclination angle can reach $\Psi_{\max} \leq 70°$ (Reid, 2010).

In the case of $\zeta = 1.2$ we focus on the GS results. Here the theoretical turn

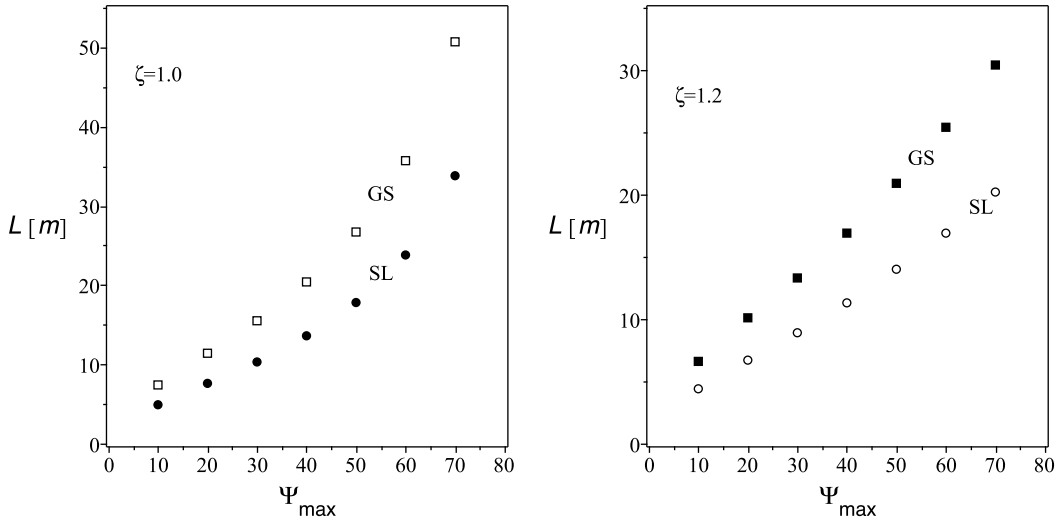

Figure 9. Distance covered in a single turn as a function of the bounce inclination angle $\Psi_{\max}$ for SL run with speed $v = 12\,\mathrm{m/s}$ and for GS run with $v = 18\,\mathrm{m/s}$. The left panel shows the results for $\zeta = 1.0$ and the right panel for $\zeta = 1.2$.

length L can also match the distance between the gates $\langle L \rangle = 26\,\mathrm{m}$ and it does so when $\Psi_{\max} \approx 60^\circ$. Unfortunately, Gilgien et al. (2015) give no information on the ski or skier inclination angles and the ski turn radius. The only other reference point is provided by the turn radius as dictated by the gate separations, $R_{\mathrm{a}} = 20\,\mathrm{m}$. In order to be consistent with the theory this radius has to be higher than the local curvature radius of the ski trajectory corresponding to $\Psi_{\max}$. Using formula (3), we find that $\Psi_{\max} = 60^\circ$ correponds to $R_{\min} = 13.5\,\mathrm{m}$, which is indeed below R_{a}.

A similar analysis of the SG and DH data shows that they cannot be explained by the pendulum model at all. For any $\Psi_{\max}$, the turn length is significantly below the mean gate separation. We anticipated this result given the fact that the gate-dictated turn radius is higher than the sidecut radius of the skis (see Table 1).

The fact that the theoretical turn length and the actual distance between the gates can be matched for some value of $\Psi_{\max}$, does not imply that the turns are wide enough to accommodate both the horizontal and fall-line separations between the gates. In order to check this, we reconstructed the trajectories of the runs corresponding to the estimated values of $\Psi_{\max}$. The top panel of Figure 10 shows the reconstruction of the SL run, which we made using $R_{\mathrm{sc}} = 15\,\mathrm{m}$, $V = 12\,\mathrm{m/s}$ from Table 1, and the turning poles of the gates with the separations $L_{\mathrm{v}} = 12\,\mathrm{m}$ and $L_{\mathrm{h}} = 4\,\mathrm{m}$ from the same table. As one can see, the agreement between the gate setting and the reconstructed trajectory is already reasonably good. We have not carried out a proper study of the parameter space in order to determine the best fit, however we have made a few additional runs and found that reducing the sidecut radius to $R_{\mathrm{sc}} = 12.7\,\mathrm{m}$ and increasing the inclination to $\Psi_{\max} = 45^\circ$ yields an even

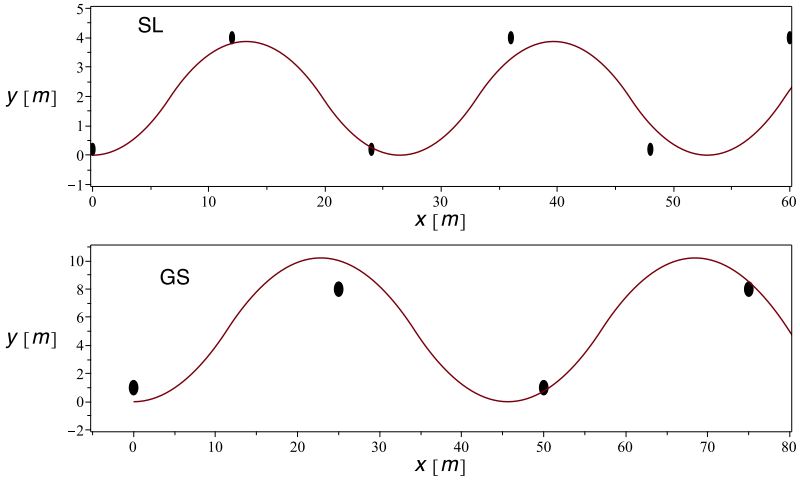

Figure 10. Simulated trajectories of SL and GS runs. The black dots indicate gates with the mean separations as in Table 1.

better fit.

The bottom panel of Figure 10 shows the similar attempted reconstruction of the GS runs of Table 1. Here we used $R_{\rm sc} = 27\,{\rm m}$, $V = 18\,{\rm m/s}$, $\Psi_{\rm max} = 62°$, $L_{\rm v} = 25\,{\rm m}$ and $L_{\rm h} = 7\,{\rm m}$. Once again, the agreement between the gate setting and the reconstructed trajectory is quite good.

Discussion and Implications

It is custom in skiing literature to talk about dynamic skiing. Usually this is done without clearly defining as to what this actually is and how it is different from the rest of skiing, presumably opposite to the dynamic one and thus static. Sometimes it is described as just fast skiing, sometimes as the one that involves high inclination angles or rapid body moves or forceful application of skis to the snow etc. Our study provides a theoretical framework that helps to clarify what may actually hide behind this somewhat intuitive and hence vague terminology. It shows that turns of alpine skiing can indeed be roughly divided into two groups depending on how balanced the skier is during their execution. We propose to call them quasi-static and dynamic turns.

In a quasi-static turn the skier is in a well-balanced position where the normal to the slope component of the gravity force is balanced by the snow reaction force and the total torque due to these and other forces is near zero as well. This position is never absolutely static because as the turn progresses the forces acting on the skier change and in order to stay in balance the skier may have to change their position. The mere fact of this change implies that the balance is not exact and hence the name quasi-static. In a dynamic turn the skier is never even close to the balance and yet the turn does not end in a crash. In order to explain the difference we need to

appeal to the properties of the centrifugal pendulum. Although we have considered only carving turns, this division is likely to be quite generic.

In our model of centrifugal pendulum, the quasi-static turns are connected to the two exceptional inclined positions of the pendulum, $\Psi = \Psi_{\rm eq}$, where the total torque vanishes. These equilibria of the pendulum are unstable and hence practically impossible. However, one can excite oscillations during which the pendulum comes close to balanced inclinations, slows down and spends quite a long time in the vicinity. The trajectory of a ski run corresponding to such oscillations is presented in Figure 8. Moreover, in contrast to the pendulum, skiers have at their disposal a range of means for stabilising their equilibria (Komissarov, 2018; Lind & Sanders, 1996; Morawski, 1973). The mathematical model of such turns has been studied in detail in Komissarov (2018). Importantly, these equilibria disappear at high speed when $V > \sqrt{gR_{\rm sc}}$ (the speed parameter $\zeta > 1$) and so does the possibility of quasi-static turns.

The dynamic turns correspond to the pendulum's oscillations about the vertical position. This vertical position is another (this time marginally stable) equilibrium of the pendulum, which naturally associates itself with straight gliding down the fall line of the slope. These oscillations have a range of possible amplitudes and periods. In fact, the period depends on the amplitude even in the small amplitude limit. This means that a whole variety of dynamic turns are allowed, both long and short. When the speed $V < \sqrt{gR_{\rm sc}}$ (the speed parameter $\zeta < 1$) there is an upper limit on the amplitude of the oscillations, which should stay below the inclination angle of the static solutions $\Psi_{\rm eq}$. Hence in this regime, the dynamic skiing is limited to relatively short turns with limited deviation from the fall line. Where to put the demarcation line between the quasi-static and dynamic turns is a matter of convention as the quasi-static solutions are also oscillations about the vertical position. Why don't the dynamic turns end in the skier hitting the ground? The pendulum model gives a very clear answer to this. As the pendulum goes over the vertical equilibrium position and is expected to start falling under the action of the gravity force, another more powerful force, the centrifugal force, takes over, slows down the fall and then pushes the pendulum back towards the vertical. In the context of skiing, the centrifugal force emerges via the ski interaction with the snow – while carving arcs in the snow the skis eventually begin to move back towards the skier body, pushing it sideways and upwards in the process.

The first turns learned by novices to the sport are quasi-static, which makes perfect sense as they do not know what to expect, lack the required skills and hence value the sense of control and balance above anything else, naturally. Even visually, the beginners appear very static. Moreover they experience great difficulty in linking their turns. This is also understandable as the transition requires to deviate from the equilibrium of the previous turn in order to reach the different equilibrium of the next turn. For example, the initiation of a new turn via relaxing of the outside leg or even lifting of the outside ski puts the skier out of balance – the pivot point of

the skier's pendulum shifts towards the inside leg whereas their CM remains where it was. The skier begins to fall to the outside of the old turn and keeps falling until the skis begin to turn, the outside becomes the inside of the new and the emerging snow reaction force reverses the fall. This simple manoeuvre requires a great deal of faith in its eventual success.

I would describe the first carving turns learned by advanced skiers also as quasi-static. For example, in one very useful drill aimed at introducing carving, a skier is instructed to start a shallow traverse, roll the skis on their inside edges and hold them in this position until they turn uphill and stop. In this drill the skier is indeed in a rather static position throughout the whole turn. Although as the turn progresses the skier's inclination angle changes a bit, this simply reflects the changing value of the balanced inclination angle (Komissarov, 2018). The first linked carving turns made by advanced skiers are also characterised by prolonged intervals of 'frozen' body position separated by relatively short transitions, indicating that the skier quickly settles to the balanced position and holds it during the turn.

During the dynamic turns skiers are subjected to significant torques. This is incompatible with the body position being 'frozen'. Instead it must be constantly changing like does the position of the oscillating pendulum. In fact, this is what is probably meant when the skiing of highly competent skiers is described as fluid. This adjective also refers to the apparent effortless and smooth nature of their movements. This fluidity has to be down to the fact that the pendulum action of the skier body does not actually require a forceful participation from the skier. The skier just has to make sure that they do not inhibit this natural process – 'get on board and enjoy the ride!'. It is long known that it is much easier to ski rhythmically – this also points to the natural pendulum action of skiing. In order to switch from one period to another the pendulum energy has to be changed, which requires an additional interaction. Hence skiers must make an extra effort if they want to change the rhythm of their turns. The advanced ski training of many ski schools includes drills specially designed to help skiers in developing the skills to do this, such as the 'slalom and traverse' drill from the set introduced on YouTube by Michaela Shiffrin (Burke Mountain Academy - Ski Drills with Mikaela Shiffrin, https://www.youtube.com/user/burkemtnacademy/playlists).

In our model, the pure gliding down the fall-line corresponds to the vertical position of the pendulum. It is not clear if this indeed the case. Indeed, any small perturbation would push the pendulum out of this position and excites vibrations instead. These vibrations correspond to skis carving shallow arcs of the sidecut radius which are only slightly deviating from the fall line. The real ski slopes are never flat and even small imperfections of their surface may play the role of such a perturbation. The vibrations can be damped due to several factors not accounted for in our basic model, including the forceful action by the skier. Moreover, it is not clear if Howe's formula (3) remains valid at small ski inclination angles. However, when one of the skis hits a rather large imperfection (e.g. a bump), this may result in a sharp

increase of its instantaneous inclination angle and hence $\Psi_{\max}$. Now this ski 'wants' to make a large arc with strong deviation from its original path, leading either to collision between the skis or their rapid separation. This must be the reason behind the horrible crashes which sometimes occur in DH and SG races during apparently innocuous straight glides.

Obviously, our pendulum model is very basic and there is room for improvements. For example, the downward vertical acceleration of skier's CM is obviously limited from above by the free-fall acceleration g whereas the downward acceleration of the pendulum weight can exceed g due to the downward component of the tension force that keeps the length of the pendulum leg unchanged. If the pivot point was not affixed to the ground but allowed to move vertically, the pendulum would lift off the ground in this regime. This discrepancy becomes significant at the high speeds and high inclination angles typical for FIS race competitions. Although in these races we do see skis lifted off the ground from time to time, this is not the norm as it is detrimental to performance. The racers use flexion of their legs to avoid these liftoffs and in the pendulum model this can be accommodated by allowing the pendulum length to vary throughout the turn. We are currently working on such a refinement of the model.

Another key simplification we wish to mention here is the assumption of the gravity force being normal to the ground, which can only be true for a slope of zero gradient ($\alpha = 0$). In fact, this is exactly the case in the setup of the ski simulator designed by SkyTechSport, Inc. (http://www.skytechsport.com). Although we do not know the exact model underpinning the design of the simulator, it is presumably quite similar to the one described here. In reality, the angle between the gravity force and the ski slope varies throughout the turn and as a result the torque due to the gravity force depends not only on the pendulum inclination but also on the angle of traverse. This can also be taken into account in a relatively straightforward way (Komissarov, 2018).

Finally, in the model there is no skier control whatsoever. Essentially, we deal with a riderless ski, where the rider is replaced by a weight attached to a ski via a rod, like a sit-ski designed for impaired skiers, and find that it can execute perfect carving turns automatically! This finding calls for a rather simple field experiment which can be used to test the theory. One has to hold the riderless ski in the vertical position until it gains enough speed and then release it, simultaneously pushing it to one side. The initial speed has to be quite high because the inclination has to stay below the balance angle $\Psi_{\rm eq} = \arcsin\zeta$. For example, if $R_{\rm sc} = 13\,{\rm m}$ and the speed is only $V = 2{\rm m/s}$ then $\zeta = 0.031$ and $\Psi_{\rm eq} = 1.8^\circ$. Not only it will be difficult to detect oscillations with the amplitude $\Psi < 1.8^\circ$, there is also a good chance that the ski will get excessively tilted either at the release or after hitting a slope imperfection, leading to a crash. The dynamics of the riderless carving ski shares some similarity with the dynamic of a riderless bike, where the centrifugal force is also the key factor preventing it from an immediate fall when going at speed (Lowel & McKell, 1982).

In real life, ski runs are constrained by terrain and obstacles. Ski racers have to negotiate gates. Hence they cannot ski in the 'autopilot' mode but need to adapt their turns accordingly. They have to decide on the length of the next turn and on its speed. In terms of the pendulum model, this could correspond to changing the pendulum energy and hence switching from one particular solution to another. Skiers have many ways of achieving this: flexing and extending their legs, changing the body angulation, forcefully pivoting the skis, changing the weight distribution between the skis etc. The issue of turn control is quite complex and needs thorough investigation.

Conclusion

In this study, we investigated the perfect carving turns of alpine skiing using the simple model of centrifugal pendulum that accounts for the actions of the gravity force and the centrifugal force associated with carving on shaped skis. The model describes two different regimes corresponding to different values of the speed parameter $\zeta = V^2/gR_{\rm sc}$. When $\zeta < 1$, there exist unstable static equilibria where the torques associated with the gravity force and the centrifugal force completely cancel each other. These solutions correspond to the quasi-static carving turns investigated in earlier studies (Jentschura & Fahrbach, 2004; Komissarov, 2018). However, the model also allows a family of completely different solutions where equilibrium is never reached and the pendulum keeps swinging from side to side. These dynamic solutions suggest that skiing in balance is not the only way of executing carving turns. Moreover, when $\zeta > 1$ the equilibria disappear altogether and only dynamic skiing is possible. Analysis of the available data on FIS alpine skiing competitions shows that during the race the elite athletes ski in this regime. We have tested the model against the mean parameters of FIS WC runs in all four classic types of alpine racing. In spite of the fact that the current pendulum model is very simplistic, it fits the data obtained for the SL and GS runs rather well. However, the model predicts the vertical acceleration which exceeds the gravitational acceleration at the summit (transition) point. This is most likely due to the assumption of the fixed pendulum length, whereas skiers actively flex and extend their legs during the turn. A study of the improved model where this restriction is relaxed is under way. The model completely disagrees with the data on SG and DH runs, presumably due to their gliding sections. More detailed quantitative studies of the real runs should help to settle this issue. The current model of centrifugal pendulum is very basic and has no feedback components associated with the skiers control over their runs. It should work very well in describing a riderless ski with a weight on a stick attached to it (e.g. a sit ski). The theory predicts that such a vehicle can execute perfect carving turns automatically. It seems relatively easy to design a field experiment aimed at testing this prediction.

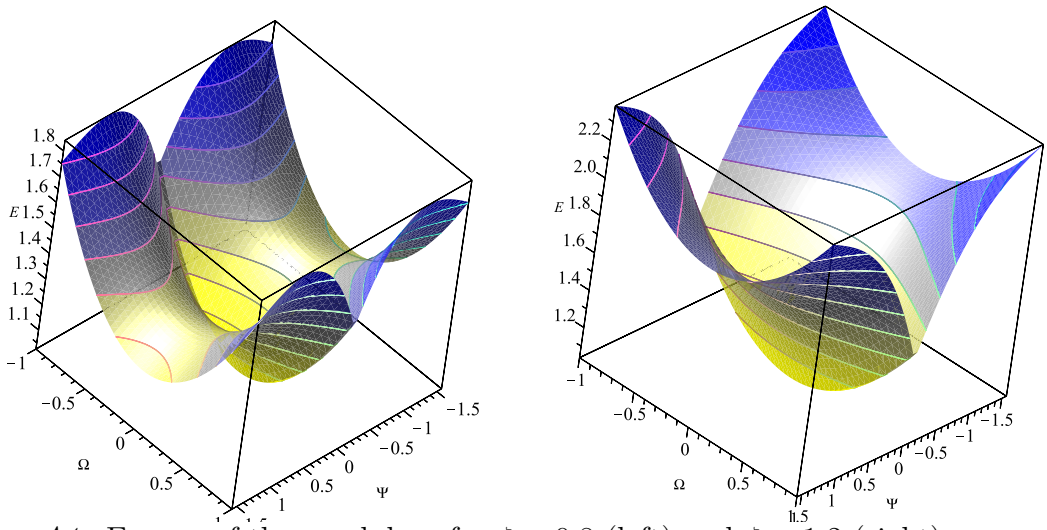

Figure A1. Energy of the pendulum for $\zeta = 0.8$ (left) and $\zeta = 1.2$ (right).

Acknowledgments

The non-trivial calculations of this study were carried out with the software package *Maple* (Maple is a trademark of Waterloo Maple Inc.).

Appendix A
Lagrangian of the basic centrifugal pendulum

It is easy to see that the Lagrangian of the centrifugal pendulum is

$$L = \frac{1}{2}\dot{\Psi}^2 - V(\Psi)\,, \tag{22}$$

where $\dot{\Psi} = d\Psi/d\tau$ and the potential energy

$$V(\Psi) = \cos\Psi + \zeta|\Psi|\,. \tag{23}$$

The conserved total energy of the pendulum is

$$E = \dot{\Psi}\frac{\partial L}{\partial \dot{\Psi}} - L = \frac{1}{2}\dot{\Psi}^2 + \cos\Psi + \zeta|\Psi|\,. \tag{24}$$

At the turning point with $\Psi_{\max}$, this yields

$$E = \cos\Psi_{\max} + \zeta|\Psi_{\max}|\,, \tag{25}$$

whereas at the summit point $\Psi = 0$ with the angular velocity $\dot{\Psi}_0$ we have

$$E = \frac{1}{2}\dot{\Psi}_0{}^2\,. \tag{26}$$

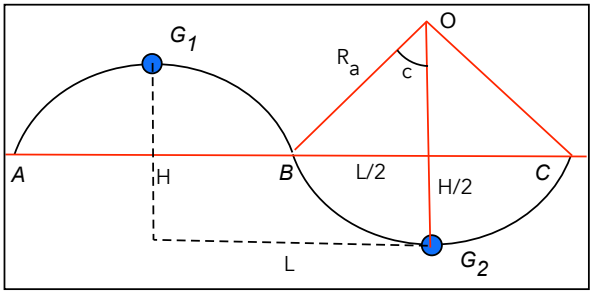

Figure B1. Fitting symmetric turn arcs.

Combining the last two results, we are able to relate $\dot{\Psi}_0$ with $\Psi_{\max}$,

$$\dot{\Psi_0}^2 = 2\left(\cos\Psi_{\max} - 1 + \zeta|\Psi_{\max}|\right) . \tag{27}$$

If $\zeta < 1$ then $E(\Psi_{\max})$ has a maximum at $\Psi_{\max} = \arcsin(\zeta)$, which corresponds to unstable equilibrium. For $\zeta > 1$ the energy is a monotonically increasing function of $\Psi_{\max}$ and no equilibrium exists.

Appendix B
Gate-dictated turn radius

Consider a set of points (the gate points) regularly spaced about a straight line (the course line). Denote the separations between two neighbouring gate points along and across the line as L and H respectively. In Figure B1 two such points are shown as thick dots G_1 and G_2. Denote as A, B and C three points on the course line that are separated by the distance L and equidistant from the orthogonal projections of the gate points to the line. Together they define two identical arcs (the turn arcs), AG_1B and BG_2C of the radius $R_{\rm a}$. From the right angle triangle shown in the figure it follows that

$$\frac{L}{2} = R_{\rm a}\sin c$$

and

$$\frac{H}{2} = R_{\rm a}(1-\cos c) .$$

Eliminating the angle c via the identity $\sin^2 c + \cos^2 c = 1$ we obtain

$$R_{\rm a} = \frac{L^2+H^2}{4H} . \tag{28}$$

The length of each arc is

$$L_{\rm a} = 2R_{\rm a}\arcsin(L/2R_{\rm a}) . \tag{29}$$

References

Coddington, E., & Levinson, N. (1955). *Theory of ordinary differential equations*. New York: McGraw-Hill.

Gilgien, M., Crivelli, P., Spörri, J., Kröll, J., & Müller, E. (2015). Characterization of course and terrain and their effect on skier speed in world cup alpine ski racing. *PLoS ONE*, *10*, e0118119.

Howe, J. (2001). *The new skiing mechanics*. Waterford, Maine: McIntire Publishing.

Jentschura, U., & Fahrbach, F. (2004). Physics of skiing: The ideal carving equation and its applications. *Can. J. Phys.*, *82*, 249.

Komissarov, S. (2018). *Modelling of carving turns in alpine skiing.* (SportRxiv. https://doi.org/10.31236/osf.io/u4ryc)

Landau, L., & Lifshitz, E. (1969). *Mechanics*. Oxford: Pergamon Press.

LeMaster, R. (2010). *Ultimate skiing*. Champaign: Human Kinetics.

Lind, D., & Sanders, S. (1996). *The physics of skiing: Skiing at the triple point*. New York: Springer-Verlag.

Lowel, J., & McKell, H. (1982). The stability of bicycles. *Americ. J. Phys.*, *50*, 1106.

Morawski, J. (1973). Control systems approach to a ski-turn analysis. *J.Biomech.*, *6*, 267.

Mössner, M., Heinrich, D., Kaps, P., Schretter, H., & Nachbauer, W. (2009). Efects of ski stiffness in a sequence of ski turns. In E. Müller, L. S., & S. T. (Eds.), *Science and skiing iv* (p. 374). Waterford, Maine: McIntire Publishing.

Reid, R. (2010). *A kinematic and kinetic study of alpine skiing technique in slalom*. PhD dissertation, Norwegian School of Sport Sciences.

Supej, M., Hebert-Losier, K., & Holmberg, H.-C. (2014). Impact of the steepness of the slope on the biomechanics of world cup slalom skiers. *Int. J. Sports Physiol. Perform.*, *10*, 361.

Yoneyama, T., Kagawa, H., & Funahashi, N. (2002). Study of the effective turn motion using a ski robot. In S. Ujihashi & H. S. J. (Eds.), *The engineering of sport 4* (p. 463). Carlton: Blackwell Publishing.